Acta Astronautica 94 (2014) 493–501

Contents lists available at ScienceDirect

Acta Astronautica

journal homepage: www.elsevier.com/locate/actaastro

Spin-axis pointing of a magnetically actuated spacecraft

G. Avanzini [a], E.L. de Angelis [b], F. Giulietti [b,*]

[a] Department of Engineering for Innovation (DII), Università del Salento, Cittadella della Ricerca, S.S. 7 km. 7+300, 72100 Brindisi, Italy
[b] Department of Industrial Engineering (DIN), Università di Bologna, Via Fontanelle 40, 47121 Forlì, Italy

ARTICLE INFO

Article history:
Received 12 July 2012
Received in revised form
17 September 2012
Accepted 24 October 2012
Available online 13 March 2013

Keywords:
Attitude control
Non-linear control
Spacecraft magnetic control
Single-axis pointing

ABSTRACT

Attitude regulation proves to be a challenging problem, when magnetic actuators alone are used as attitude effectors, since they do not provide three independent control torque components at each time instant. In this paper a rigorous proof of global exponential stability is derived for a magnetic control law that leads the satellite to a desired spin condition around a principal axis of inertia, pointing the spin axis toward a prescribed direction in the inertial frame. The technique is demonstrated by means of numerical simulation of a few example maneuvers. An extensive Monte Carlo simulation is performed for random initial conditions, in order to investigate the effect of changes in control law gains.

1. Introduction

The objective of this study is the determination of a control law that allows for the acquisition of a desired pure spin condition of a rigid spacecraft around one of its principal axes of inertia by means of magnetic actuators only, while aiming the spin axis in a prescribed direction in the inertial space. The use of magnetic actuators on satellites flying low earth orbits (LEOs) poses several problems in the selection of suitable control strategies because of the fact that the interaction between the local geomagnetic field and the coils generates torques that lie on a plane that is orthogonal to the magnetic field itself. This makes the system inherently underactuated, with the inability to provide three independent control torques at each time instant. As a consequence, the application of well known control strategies is no longer possible in this case for both regulation and tracking of desired attitudes.

The interest in magnetic actuators is due to different reasons [1]. First of all, savings in weight, cost and complexity with respect to other systems are significant. At the same time, the possibility of a smooth modulation of control torques greatly limits the interaction of the attitude control system with flexible modes. In spite of the presence of only two magnetic control components, attitude stabilization is possible because, on average, the system proves to be controllable if the orbit possesses an adequate inclination with respect to the geomagnetic equator [2]. This mechanism is based on the fact that the magnetic field vector periodically rotates over inclined orbits as the spacecraft completes its movement around the Earth, making the problem intrinsically time-varying.

Thrusters allow for a faster angular momentum dumping, but this comes at the cost of large propellant consumption and the added complexity of a fuel system (tanks, pipes, valves, etc.) feeding a minimum of eight thrusters required for full three-axis control. Moreover, pulse modulation may cause strong interactions of attitude dynamics with fuel sloshing and flexible modes, thus harming pointing precision [3]. When momentum and reaction wheels are used, for example in large satellites with stringent pointing requirements, the need of redundancy and the presence of high spin-rate elements make the system more complex, heavy and prone

* Corresponding author. Tel.: +39-0543-374-424; fax: +39-0543-374-477.
E-mail address: fabrizio.giulietti@unibo.it (F. Giulietti).

0094-5765/$ - see front matter © 2013 Published by Elsevier Ltd. on behalf of IAA.
http://dx.doi.org/10.1016/j.actaastro.2012.10.035

to (possibly multiple) failure(s). In addition, the problem of wheel desaturation arises when the effects of environmental torques need to be compensated, so that other means are needed to unload the wheel cluster, such as thrusters or magnetic torquers [4,5].

When three independent control torques are available, the problem of attitude control can be conveniently expressed in terms of Euler axis/angle, where a nominal Euler axis rotation directly takes the spacecraft from an initial attitude to a desired final one by means of the minimum angular path. This maneuver strategy can be implemented by means of a quaternion feedback control [6]. If, on the converse, the spacecraft is underactuated, e.g. when magnetic torquers are the only attitude effectors available, the nominal rotation cannot be performed.

Different approaches have been investigated in the past for tackling the problem of control in underactuated conditions [7,8], which represent an interesting solution also as a strategy for failure mitigation systems (e.g. after loss of a reaction wheel in a three-axes stabilized spacecraft with no redundancy) [9–11], possibly at the cost of reduced closed-loop performance in terms of pointing accuracy and/or maneuver time. In [12] it is shown that a feasible rotation always exists around a non-nominal Euler axis that lies on the plane perpendicular to the torqueless direction and allows for exact pointing of a given body-fixed axis toward any prescribed target direction.

Such a capability may be useful in several mission scenarios. As an example, Earth pointing may be required in the case of Earth observation, with the accurate alignment of the boresight of a sensor payload. This is the case of ALMASat-EO, a microsatellite under development at the University of Bologna, mounting an innovative multispectral camera and testing a novel micropropulsion system for orbit control [13]. In other cases accurate pointing may be required for communication purposes with a directional antenna. Another application may be finally represented by the orientation of a thruster nozzle for precise orbit maneuvers, where the accuracy must lie within a fraction of a degree.

In Cheon et al. [14], the problem of target pointing is tackled in the case where only magnetic devices are used, more specifically magnetometers and magnetic torquers, with the function, respectively, of attitude sensors and actuators. As a major limitation, the approach, derived after a linearization of the governing equations of motion, provides local asymptotic stability only for the resulting controller. In [15] a pointing control law is proven to asymptotically stabilize an axisymmetric spacecraft under controller saturation and multiple failures of up to two magnetic torque-rods, with good numerical results also extended to satellites with triaxial inertia properties.

In this paper a continuous magnetic torque command is proposed that leads a three-inertial spacecraft to a desired spin condition around a principal axis of inertia that is aligned toward a target direction, fixed in the inertial reference frame. A simple control law based on angular momentum shaping successfully achieves the mission task. The analysis follows the approach introduced in [16], where convergence toward a desired spin rate was proven by demonstrating robustness of global exponential stability (GEAS) of a nominal system by means of generalized exponential asymptotic stability in variations (GEASVs) tools [17,18]. In this framework, the error dynamics equation is first derived for two error signals, namely the angular momentum error in the body frame and the angular momentum error with respect to the desired direction of the spin axis in the inertial frame. The error dynamics can be cast in the classical form of a nominal system perturbed by a vanishing perturbation term. Then, after proving the generalized exponential stability for the nominal system, such result is extended to the perturbed system [19].

The control law is then tested by means of numerical simulations, in order to demonstrate performance and stability characteristics of the method. In particular, a Monte Carlo approach is used to empirically evaluate the convergence capability of the controller to obtain single-axis pointing from arbitrary initial conditions and determine average convergence time as a function of control gains.

2. Mathematical preliminaries

The dynamic model of a rigid satellite expressed in a set of principal axes of inertia, $\mathbb{F}_B=\{P;\hat{\boldsymbol{e}}_1,\hat{\boldsymbol{e}}_2,\hat{\boldsymbol{e}}_3\}$, centered in the spacecraft center of mass P, is given by Euler equation

$$\dot{\boldsymbol{h}}=\boldsymbol{M}-\boldsymbol{\omega}\times\boldsymbol{h} \tag{1}$$

where $\boldsymbol{h}=(h_1,h_2,h_3)^T=\boldsymbol{J}\boldsymbol{\omega}$ is the absolute angular momentum vector represented in terms of components in the body-fixed frame, $\mathbb{F}_B$, $\boldsymbol{\omega}=(\omega_1,\omega_2,\omega_3)^T$ is the absolute velocity vector, $\boldsymbol{J}=\mathrm{diag}(J_1,J_2,J_3)$ is the spacecraft inertia matrix, and $\boldsymbol{M}=\boldsymbol{M}^{(c)}+\boldsymbol{M}^{(d)}$ is the external torque vector, given by the sum of control and disturbance torques, respectively. No external disturbances will be considered in the present analysis (that is, $\boldsymbol{M}^{(d)}=\boldsymbol{0}$).

For a spacecraft controlled by means of three mutually orthogonal magnetic coils, the control torque generated by the magnetorquers is given by

$$\boldsymbol{M}^{(c)}=\boldsymbol{m}\times\boldsymbol{b} \tag{2}$$

where $\boldsymbol{m}$ is the commanded magnetic dipole moment vector generated by the coils and $\boldsymbol{b}=\mathbb{T}_{BO}\boldsymbol{b}_O$ is the local geomagnetic field vector expressed in terms of body-frame components.

A circular low earth orbit of radius r_c, period T_{orb}, and orbit rate $\Omega=2\pi/T_{orb}$ is considered. The components $\boldsymbol{b}_O$ of the geomagnetic field are expressed in the local-vertical/local-horizontal orbit frame, $\mathbb{F}_O$, by means of a simple tilted dipole model [20,21], where the z_O-axis lies along the local vertical, the y_O-axis is normal to the orbit plane, in a direction opposite to the orbital angular speed $\boldsymbol{\omega}^{orb}$, and the transverse axis x_O completes a right-handed triad, in the direction of the orbital velocity. The geometry of the problem is sketched in Fig. 1.

The coordinate transformation matrix between $\mathbb{F}_O$ and $\mathbb{F}_B$

$$\mathbb{T}_{BO}=(\bar{q}^{\,2}-\boldsymbol{q}^T\boldsymbol{q})\mathbb{I}_3+2\boldsymbol{q}\boldsymbol{q}^T-2\bar{q}\,\tilde{\mathbb{Q}} \tag{3}$$

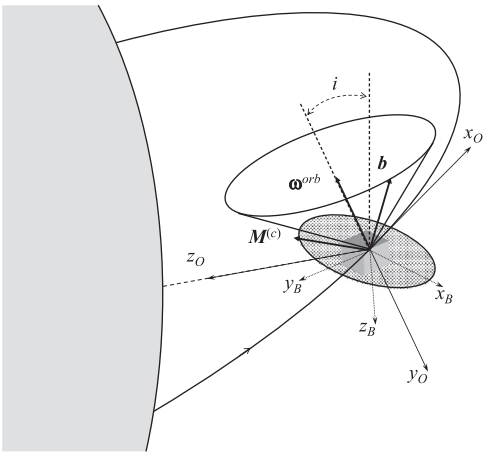

Fig. 1. Geometry of the problem.

is expressed as a function of the unit quaternion $\mathbf{Q}=(\boldsymbol{q}^T,\overline{q})^T$, that represents satellite's attitude with respect to the orbit frame. In Eq. (3), $\mathbb{I}_3$ is the 3×3 identity matrix and $\tilde{\mathbb{Q}}$ is the skew symmetric matrix equivalent to the cross product, such that $\tilde{\mathbb{Q}}\,\boldsymbol{v}=\boldsymbol{q}\times\boldsymbol{v}$, for any $\boldsymbol{v}\in\mathbb{R}^3$.

The unit quaternion evolves as a function of the angular speed of the spacecraft relative to $\mathbb{F}_O$, given by $\boldsymbol{\omega}^r=\boldsymbol{\omega}-\mathbb{T}_{BO}\,\boldsymbol{\omega}_O^{orb}$, where $\boldsymbol{\omega}_O^{orb}=(0,-\Omega,0)^T$ is the angular speed of $\mathbb{F}_O$ with respect to an inertial frame [22].

The kinematics of $\mathbf{Q}$ is given by

$$\dot{\boldsymbol{q}}=\tfrac{1}{2}(\overline{q}\,\boldsymbol{\omega}^r-\boldsymbol{\omega}^r\times\boldsymbol{q})$$

$$\dot{\overline{q}}=-\tfrac{1}{2}\boldsymbol{\omega}^{rT}\boldsymbol{q} \tag{4}$$

3. Acquisition of a pure spin condition in the inertial frame

Let $\hat{\boldsymbol{\sigma}}$ be the unit vector that identifies the target direction which is fixed in the inertial frame, and $\boldsymbol{\omega}_d$ is the desired pure spin condition about one of the principal axes of inertia, *e.g.* $\boldsymbol{\omega}_d=(0,\overline{\omega}_d,0)^T$. The components of the desired angular momentum vector, expressed in a set of principal axes and in the inertial frame, are given by $\boldsymbol{h}_d=\boldsymbol{J}\,\boldsymbol{\omega}_d$ and $\boldsymbol{H}_d=\|\boldsymbol{h}_d\|\hat{\boldsymbol{\sigma}}$, respectively. Two different angular momentum error variables can thus be introduced, namely

$$\boldsymbol{\zeta}=\boldsymbol{H}_d-\boldsymbol{h} \tag{5}$$

and

$$\boldsymbol{\varepsilon}=\boldsymbol{h}_d-\boldsymbol{h} \tag{6}$$

where all the vector quantities, including $\boldsymbol{H}_d$, are represented in terms of body-frame components. Finally $\hat{\boldsymbol{b}}=\boldsymbol{b}/\|\boldsymbol{b}\|$ is the unit vector parallel to the geomagnetic field.

The scope of this section is to prove that, on inclined LEOs, the control law

$$\boldsymbol{M}^{(c)}=(\mathbb{I}_3-\hat{\boldsymbol{b}}\hat{\boldsymbol{b}}^T)(k_\zeta\boldsymbol{\zeta}+k_\varepsilon\boldsymbol{\varepsilon}) \tag{7}$$

with $k_\zeta>0$ and $k_\varepsilon>0$, drives the spacecraft toward a pure spin condition about one of the principal axes of inertia (i.e. $\boldsymbol{\varepsilon}\to\mathbf{0}$), while pointing the spin axis along the target direction $\hat{\boldsymbol{\sigma}}$ (i.e. $\boldsymbol{\zeta}\to\mathbf{0}$), despite the fact that the resulting control torque, perpendicular to $\hat{\boldsymbol{b}}$, does not provide full actuation.

Since $\boldsymbol{H}_d$ is fixed in the inertial frame, its dynamics is given in body coordinates by

$$\dot{\boldsymbol{H}}_d=-\boldsymbol{\omega}\times\boldsymbol{H}_d \tag{8}$$

By recalling the definition of the error one has

$$\dot{\boldsymbol{\zeta}}=-\boldsymbol{M}^{(c)}-\boldsymbol{\omega}\times\boldsymbol{\zeta} \tag{9}$$

From Eq. (6) it immediately follows that

$$\boldsymbol{\omega}=\boldsymbol{J}^{-1}(\boldsymbol{h}_d-\boldsymbol{\varepsilon}) \tag{10}$$

that can be substituted in Eq. (9). By taking into account Eq. (7), one has

$$\dot{\boldsymbol{\zeta}}=-(\mathbb{I}_3-\hat{\boldsymbol{b}}\hat{\boldsymbol{b}}^T)(k_\zeta\boldsymbol{\zeta}+k_\varepsilon\boldsymbol{\varepsilon})-\boldsymbol{J}^{-1}(\boldsymbol{h}_d-\boldsymbol{\varepsilon})\times\boldsymbol{\zeta} \tag{11}$$

Since $\boldsymbol{h}_d$ is a constant vector in body axes and taking into account Eq. (10), the body frame angular momentum error dynamics achieves the form

$$\dot{\boldsymbol{\varepsilon}}=-(\mathbb{I}_3-\hat{\boldsymbol{b}}\hat{\boldsymbol{b}}^T)(k_\zeta\boldsymbol{\zeta}+k_\varepsilon\boldsymbol{\varepsilon})+\boldsymbol{J}^{-1}(\boldsymbol{h}_d-\boldsymbol{\varepsilon})\times(\boldsymbol{h}_d-\boldsymbol{\varepsilon}) \tag{12}$$

The formulation of the spin axis pointing problem turns out to be remarkably simpler if error dynamics is represented in terms of components in the inertial frame, $\mathbb{F}_I$, rather than in the body frame, $\mathbb{F}_B$. With this choice, the dynamics of the angular momentum errors in Eqs. (11) and (12) can be respectively written as

$$\dot{\boldsymbol{Z}}=-\mathbb{T}_{BI}^T(\mathbb{I}_3-\hat{\boldsymbol{b}}\hat{\boldsymbol{b}}^T)\mathbb{T}_{BI}(k_\zeta\boldsymbol{Z}+k_\varepsilon\boldsymbol{E}) \tag{13}$$

$$\dot{\boldsymbol{E}}=-\mathbb{T}_{BI}^T(\mathbb{I}_3-\hat{\boldsymbol{b}}\hat{\boldsymbol{b}}^T)\mathbb{T}_{BI}(k_\zeta\boldsymbol{Z}+k_\varepsilon\boldsymbol{E})-\mathbb{T}_{BI}^T(\boldsymbol{J}^{-1}\mathbb{T}_{BI}\boldsymbol{E}\times\boldsymbol{h}_d) \tag{14}$$

where $\mathbb{T}_{BI}$ is the coordinate transformation matrix between $\mathbb{F}_I$ and $\mathbb{F}_B$, such that $\boldsymbol{Z}=\mathbb{T}_{BI}^T\boldsymbol{\zeta}$ and $\boldsymbol{E}=\mathbb{T}_{BI}^T\boldsymbol{\varepsilon}$. Given $\boldsymbol{Y}=(\boldsymbol{Z}^T,\boldsymbol{E}^T)^T$, $\boldsymbol{Y}\in\mathbb{R}^6$, the system in Eqs. (13) and (14) can be reshaped into

$$\dot{\boldsymbol{Y}}=-\boldsymbol{A}(t)\boldsymbol{K}\boldsymbol{Y}-\boldsymbol{B}(\boldsymbol{Y}) \tag{15}$$

where

$$\boldsymbol{A}(t)=\begin{pmatrix}\mathbb{T}_{BI}^T(\mathbb{I}_3-\hat{\boldsymbol{b}}\hat{\boldsymbol{b}}^T)\mathbb{T}_{BI} & \mathbb{T}_{BI}^T(\mathbb{I}_3-\hat{\boldsymbol{b}}\hat{\boldsymbol{b}}^T)\mathbb{T}_{BI}\\ \mathbb{T}_{BI}^T(\mathbb{I}_3-\hat{\boldsymbol{b}}\hat{\boldsymbol{b}}^T)\mathbb{T}_{BI} & \mathbb{T}_{BI}^T(\mathbb{I}_3-\hat{\boldsymbol{b}}\hat{\boldsymbol{b}}^T)\mathbb{T}_{BI}\end{pmatrix} \tag{16}$$

is the actuation matrix, $\boldsymbol{A}\in\mathbb{R}^{6\times 6}$

$$\boldsymbol{K}=\begin{pmatrix}k_\zeta\mathbb{I}_3 & \mathbf{0}_{3\times 3}\\ \mathbf{0}_{3\times 3} & k_\varepsilon\mathbb{I}_3\end{pmatrix} \tag{17}$$

is the gain matrix, $\boldsymbol{K}\in\mathbb{R}^{6\times 6}$, and

$$\boldsymbol{B}(\boldsymbol{Y})=\begin{pmatrix}\mathbf{0}_{3\times 1}\\ \mathbb{T}_{BI}^T[\boldsymbol{J}^{-1}\mathbb{T}_{BI}(Y_4,Y_5,Y_6)^T\times\boldsymbol{h}_d]\end{pmatrix} \tag{18}$$

is a term related to gyroscopic coupling effects.

The system in the form of Eq. (15) matches the classical perturbed system structure $\dot{\boldsymbol{Y}}=\boldsymbol{f}(t,\boldsymbol{Y})+\boldsymbol{g}(t,\boldsymbol{Y})$, where $\boldsymbol{f}(t,\boldsymbol{Y})=-\boldsymbol{A}(t)\boldsymbol{K}\,\boldsymbol{Y}$ governs the nominal system and $\boldsymbol{g}(t,\boldsymbol{Y})=-\boldsymbol{B}(\boldsymbol{Y})$ is a vanishing perturbation term.

Definition 1. The solution $\boldsymbol{x}=\mathbf{0}$ of the system $\dot{\boldsymbol{x}}=\boldsymbol{f}(t,\boldsymbol{x})$ is said to be generalized exponentially asymptotically stable

in variation (GEASV) if

$$\|\boldsymbol{\Phi}(t,t_0,\boldsymbol{x}_0)\| \le k(t)\, e^{\,p(t_0)-p(t)} \tag{19}$$

for $t \ge t_0 \ge 0$, where $\boldsymbol{\Phi}(t,t_0,\boldsymbol{x}_0) = \partial \boldsymbol{x}(t,t_0,\boldsymbol{x}_0)/\partial \boldsymbol{x}_0$ is the fundamental matrix, $\boldsymbol{x}_0 = \boldsymbol{x}(t_0)$, $k > 0$ is continuous on $\mathbb{R}^+$, and $p \in C(\mathbb{R}^+)$, $p(0) = 0$, is strictly increasing in $t \in \mathbb{R}^+$.

Proposition 1. *The origin $\boldsymbol{Y} = \boldsymbol{0}$ is a generalized exponentially asymptotically stable in variation (GEASV) equilibrium point of the nominal system $\dot{\boldsymbol{Y}} = \boldsymbol{f}(t,\boldsymbol{Y})$.*

Proof. The origin $\boldsymbol{Y} = \boldsymbol{0}$ is a globally exponentially stable equilibrium point of the nominal system (see Appendix), then there exist constants $k_1 > 0$, and $\lambda_1 > 0$ such that

$$\|\boldsymbol{Y}(t,t_0,\boldsymbol{Y}_0)\| \le k_1 \|\boldsymbol{Y}_0\| e^{-\lambda_1 (t-t_0)} \tag{20}$$

for $t \ge t_0 \ge 0$. The nominal system is linear time varying, and its solution takes the form $\boldsymbol{Y}(t,t_0) = \boldsymbol{\Phi}(t,t_0)\boldsymbol{Y}_0$, where $\boldsymbol{\Phi}(t,t_0) \in \mathbb{R}^{6\times 6}$ is the fundamental matrix. Thus, there exist constants $k_2 > 0$, and $\lambda_2 > 0$ such that

$$\|\boldsymbol{\Phi}(t,t_0)\| \le k_2\, e^{-\lambda_2 (t-t_0)} \tag{21}$$

By choosing small values for a constant $\lambda_3 > 0$, and sufficiently large values of $k(t) = k_3 =$ const., the definition in Eq. (19) is finally tailored to the present case with the function $p(t) = \lambda_3 t^c$

$$\|\boldsymbol{\Phi}(t,t_0)\| \le k_3 e^{-\lambda_3 (t^c - t_0^c)} \tag{22}$$

for some $c > 1$. Note that GEASV implies global exponential stability [17].

Global exponential stability of the system (15) is provided by the following theorem [19].

Theorem 1. *Given the perturbed system $\dot{\boldsymbol{x}} = \boldsymbol{f}(t,\boldsymbol{x}) + \boldsymbol{g}(t,\boldsymbol{x})$, let the origin $\boldsymbol{x} = \boldsymbol{0}$ be a GEASV solution of the nominal system $\dot{\boldsymbol{x}} = \boldsymbol{f}(t,\boldsymbol{x})$, and the perturbed term satisfy $\|\boldsymbol{g}(t,\boldsymbol{x})\| \le \varphi(t)\|\boldsymbol{x}\|$, $\varphi \in C(\mathbb{R}^+)$, $t \ge t_0 \ge 0$, $\|\boldsymbol{x}\| < \infty$. If the maximal solution of the scalar differential equation*

$$\dot{u} = [-\dot{p}(t) + \varphi(t)]\, K(t) u, \quad u(t_0) \ge 0, \tag{23}$$

where $p(t)$ and $k(t)$ are the functions from the definition of GEASV, is GEASV, then every solution of the perturbed system is GEASV.

The proof is found in [19] (see Theorem 3.8).

Remark. For spin stabilization about the y-axis, hypotheses of Theorem 1 are satisfied. As a matter of fact, with the choice of $p(t) = \lambda_3 t^c$, $c > 1$, and $k(t) = k_3 =$ const. in Eq. (22), the differential problem of Eq. (23) becomes:

$$\dot{u} = \left(-c\lambda_3 t^{c-1} + \frac{J_2}{J_{min}} |\overline{\omega}_d| \right) k_3 u, \quad u_0 = u(t_0) \ge 0 \tag{24}$$

where J_{min} is the minimum moment of inertia. The solution to the Eq. (24)

$$u(t) = u_0 \exp\left\{ k_3 \left[\left(\lambda_3\, t_0^c - \frac{J_2}{J_{min}} |\overline{\omega}_d| t_0 \right) - \left(\lambda_3\, t^c - \frac{J_2}{J_{min}} |\overline{\omega}_d| t \right) \right] \right\} \tag{25}$$

is governed by a fundamental function

$$\Phi(t,t_0) = \exp\left\{ k_3 \left[\left(\lambda_3 t_0^c - \frac{J_2}{J_{min}} |\overline{\omega}_d| t_0 \right) - \left(\lambda_3 t^c - \frac{J_2}{J_{min}} |\overline{\omega}_d| t \right) \right] \right\} \tag{26}$$

which, in conclusion, satisfies the definition of GEASV in Eq. (19) with $k(t) = k_4 =$ const. and $p(t) = \lambda_4 t^c$, for some constants $k_4 > k_3$, and $0 < \lambda_4 < \lambda_3$.

As a final issue, it is important to discuss the effects of uncertainties on the magnetic field on expected performance of the control law, where the actual geomagnetic vector, $\tilde{\boldsymbol{b}} = \boldsymbol{b} + \Delta\boldsymbol{b}$, can be written as the sum of its ideal (or estimated) value $\boldsymbol{b}$ plus an uncertainty, $\Delta\boldsymbol{b}$. The commanded dipole moment $\boldsymbol{m} = \boldsymbol{b} \times \boldsymbol{M}/\|\boldsymbol{b}\|^2$ is evaluated as in [23], for the nominal values of geomagnetic field vector, $\boldsymbol{b}$, and control torque, $\boldsymbol{M} = (\mathbb{I}_3 - \hat{\boldsymbol{b}}\hat{\boldsymbol{b}}^T)(k_\zeta \boldsymbol{\zeta} + k_\varepsilon \boldsymbol{\varepsilon})$. The actual control torque, $\tilde{\boldsymbol{M}} = \boldsymbol{m} \times \tilde{\boldsymbol{b}}$, thus achieves the form

$$\tilde{\boldsymbol{M}} = [(\boldsymbol{b}^T \tilde{\boldsymbol{b}})\boldsymbol{M} - (\boldsymbol{M}^T \tilde{\boldsymbol{b}})\boldsymbol{b}]/\|\boldsymbol{b}\|^2$$

A condition on the maximum acceptable deviation for the magnetic field with respect to its nominal value assumed in the derivation of the control law can be found, such that asymptotic convergence to the desired spin condition can be obtained also in the presence of an uncertain geomagnetic field. Noting that $\boldsymbol{m}$, $\boldsymbol{b}$, and $\boldsymbol{M}$ are mutually perpendicular, the uncertainty on the geomagnetic field can be represented in terms of components parallel to $\boldsymbol{m}$, $\boldsymbol{b}$, and $\boldsymbol{M}$, respectively, that is, $\Delta\boldsymbol{b} = (\Delta b_m, \Delta b_b, \Delta b_M)^T$. The first component of the uncertainty does not affect the actual torque at all, whereas the second one, which varies the magnitude of $\boldsymbol{b}$, affects the magnitude of the resulting torque only, but it does not change its direction, and it is thus equivalent to a variation of the gains, k_ε and k_ζ. Both these perturbations of $\boldsymbol{b}$ can thus be rather large, without consequences on the stability of the control law, and Δb_M is the only uncertainty component that needs to be bounded.

When only Δb_M is considered, $\tilde{\boldsymbol{b}}$ is rotated by an angle δ with respect to its nominal direction $\boldsymbol{b}$ in the plane identified by $\boldsymbol{b}$ and $\boldsymbol{M}$, such that $(\boldsymbol{b}^T\tilde{\boldsymbol{b}})/\|\boldsymbol{b}\|^2 \approx \cos\delta$, with $\tan\delta = \Delta b_M/\|\boldsymbol{b}\|$. The direction of the error signal, $\boldsymbol{e} = k_\zeta \boldsymbol{\zeta} + k_\varepsilon \boldsymbol{\varepsilon}$ also lies on the plane identified by $\boldsymbol{M}$ and $\boldsymbol{b}$, forming an angle β with $\boldsymbol{b}$. Assuming for the sake of simplicity that the gains k_ε and k_ζ are equal ($k_\varepsilon = k_\zeta = k$), the nominal control torque is given by $\|\boldsymbol{M}\| = k\|\boldsymbol{\varepsilon} + \boldsymbol{\zeta}\| \sin\beta$. At this point it is possible to show that the dot product represented by $\boldsymbol{e}^T\tilde{\boldsymbol{M}}$ remains positive if $\delta < \beta$, that is, the magnitude of the error signal decreases thanks to the considered control law in spite of the uncertainty on $\boldsymbol{b}$. This translates into a requirement on the maximum admissible value for Δb_M, that is required to satisfy the inequality $\Delta b_M/\|\boldsymbol{b}\| = \tan\delta < \tan\beta$.

The sum of the error signals $\boldsymbol{\varepsilon}$ and $\boldsymbol{\zeta}$ can, in general, achieve any value, and β can thus become arbitrarily small. In this condition, the robustness requirement on the exact estimate of $\boldsymbol{b}$ appears as a severe one. But when the error signal is close to the nominal direction of $\boldsymbol{b}$, the corresponding nominal torque, proportional to $\sin\beta$, is also small. In such a case, errors on the control action do not affect significantly convergence performance, which becomes only marginally slower. Moreover, the choice of the control gains requires that the error signal is maintained as much as possible far from the direction of the magnetic field, as suggested in [16] and [23]. In any case, provided that it is not possible to activate magnetic coils

during the measurement of $\boldsymbol{b}$ with magnetometers, it is possible to exploit intervals during which the angle β becomes small in order to switch the control law off and activate magnetometers to update the estimate of $\boldsymbol{b}$.

4. Results and discussion

The control law proposed in the previous section for the acquisition of the desired pure spin condition and the desired orientation of the spin axis is now applied to a low earth orbit micro-satellite [13], equipped with three mutually orthogonal magnetic coils ($\overline{m}_1 = \overline{m}_2 = \overline{m}_3$). Table 1 shows spacecraft data and orbit parameters. The angle α, defined as

$$\alpha = \cos^{-1}(\hat{\boldsymbol{\sigma}} \cdot \hat{\boldsymbol{e}}_2) \tag{27}$$

that represents the angular distance between the desired spin axis $\hat{\boldsymbol{e}}_2$ and the target direction $\hat{\boldsymbol{\sigma}}$, will be used as a measure of the misalignment.

A set of Monte Carlo simulations is performed in order to investigate merit functions, such as convergence time and electrical power consumption, as a function of control law gains k_ζ and k_ε for randomly chosen initial conditions representative of the (at least partially) unknown tumbling motion of the payload after its ejection from the upper stage of the rocket launcher and the attitude and phase along the orbit at which the spin maneuver is started.

Initial conditions are determined by means of the psuedo-random number generator, rand(), implemented in Matlab™ environment. In particular, initial angular rates are generated, so that the same amount of angular momentum $\|\Delta\boldsymbol{h}_0\|$ is dissipated for each test case of the Monte Carlo simulation [23], where

$$\|\Delta\boldsymbol{h}_0\| = \max_{i\in\{1,2,3\}} (J_i)\omega_{ref} \tag{28}$$

with $\omega_{ref} = 1$ rad/s, and $\Delta\boldsymbol{h}_0 = \boldsymbol{h}_d - \boldsymbol{h}_0$, $\boldsymbol{h}_0 = \boldsymbol{h}(t_0)$ being the angular momentum vector at the initial time, t_0. The desired spin condition is represented by a desired angular rate $\overline{\omega}_d = 0.110$ rad/s about $\hat{e}_2$, aligned with the orbit normal $\hat{\boldsymbol{y}}_O$.

As a last issue of practical relevance, an estimate of the maneuver cost is provided in terms of electrical power consumption. A maximum magnetic dipole $m_{\max} = 3$ A m^2 is assumed for each of the torque-rods, its actual value being proportional to the current absorbed. The total electrical energy, $\mathcal{E}$, necessary for completing the maneuver is thus proportional to

$$\mathcal{E} \propto E = \int_0^{t_F} \left(\sum_{i=1}^{3} |m_i| \right) \mathrm{d}t \tag{29}$$

Fig. 2 shows the results obtained from the first set of Monte Carlo simulations, performed over a population of 1000 test cases, where performance in terms of time and energy consumption are reported for different values of the gain k, when $k_\varepsilon = k_\zeta = k$. The value t_F indicates the number of orbits necessary to dissipate the angular momentum in excess of the commanded value and reach the desired spin condition. A value of 99.99% of the initial error on angular momentum, assumed equal for all the test cases, was chosen as the threshold for a sufficiently small residual error, with $\|\boldsymbol{\zeta}\| < 10^{-4} \cdot \|\Delta\boldsymbol{h}_0\|$. For each performance parameter, average value and standard deviation are reported, the latter providing an indication of the dispersion of the results.

In the first set of Monte Carlo simulations, the best performance in terms of average convergence time is obtained for $k = k_{t_{min}} = 0.004$, that represents a minimum for t_F in Fig. 2 for ALMASat–EO. This behavior can be explained as in [23]. On one side, when the gain is too small, the maneuver becomes slower, because one does not fully exploit the available control power for a long portion of the final convergence. At the same time, when the gain is too large, the error component in the direction normal to the geomagnetic field would be rapidly canceled, thus leaving the angular momentum error vector parallel to $\hat{\boldsymbol{b}}$, that is, parallel to the underactuated direction along which no control action is available. This makes the convergence very slow, inasmuch as it relies on the (indeed) slow motion of the geomagnetic field in the orbital frame.

When the spacecraft is required to achieve a desired pure spin condition with no constraints on the direction of the spin axis, it is possible to estimate a reasonable order of magnitude for the gain k_ε on the basis of a sequence of inequalities that provide an upper bound to k_ε [16]. The actual optimal value is thus expected to be smaller than its bound, $k_\varepsilon = \overline{\omega}_d$. In the present case, the optimal gain appears to be one order of magnitude smaller than the suggested value obtained from the rule

Table 1
Spacecraft and orbit data, with initial conditions for a sample maneuver.

Parameter	Symbol	Value	Units
Spacecraft data			
Principal moments of inertia	J_1, J_2, J_3	0.951, 0.970, 0.946	kg m^2
Maximum magnetic dipole	$m_{\max}$	3	A m^2
Orbit data			
Radius	r_c	7064	km
Period	T_{orb}	5909	s
Inclination	i	98	deg
Sample maneuver			
Initial conditions	$\boldsymbol{\omega}_0$	$(0.3678, 0.8732, 0.5498)^T$	rad/s
	$\mathbf{Q}_0$	$(-0.3009, 0.2263, 0.2813, 0.8827)^T$	

of thumb discussed in [16] for the simple pure spin acquisition case (without pointing).

As for the energy necessary to achieve the desired spin condition, note that it monotonically increases with k. This makes that sub-optimal performance in terms of convergence time to be considered as acceptable in all those cases when significant savings in terms of electrical energy consumption result into smaller and lighter systems of batteries.

A typical example of the behavior of the pointing error α is reported in Fig. 3, together with the variation of three components of the angular rate vector $\boldsymbol{\omega}$ (Fig. 4) for $k_\varepsilon = k_\zeta = 0.004$, starting from the randomly chosen initial angular rate $\boldsymbol{\omega}_0$ and attitude $\mathbf{Q}_0$ reported in Table 1, that correspond to a pointing error of about 50 deg between $\hat{\boldsymbol{e}}_2$ and the orbit normal.

During the initial phase of the detumbling, when the angular rate is high, the pointing error of the desired spin axis with respect to the prescribed inertial direction (that is, $\hat{\boldsymbol{e}}_2$ and the normal to the orbit plane, respectively, in the considered example) exhibits a high frequency oscillation, where the frequency is related to the angular speed. For $0 < t/T_{orb} < 1$, the coils work at saturation and the control law is, in practice, similar to a switching control logic, simply aimed at reducing the angular rate. Once the tumbling motion is slowed, the oscillation of the pointing error is rapidly reduced ($t/T_{orb} > 1.1$) and its behavior transformed into an almost monotonous convergence toward zero for $t/T_{orb} > 1.4$.

A second set of Monte Carlo simulations is performed in order to analyze the effects of variations of the ratio k_ε/k_ζ, i.e. different weightings between the control actions that lead the satellite to the desired spin, respectively, in the body-frame and in the inertial-frame. Fig. 5 gives a graphical representation of the results in terms of average convergence time and electrical energy consumption parameter when the ratio k_ε/k_ζ is varied between 0.1 and 10. The ratio is varied, while keeping the sum of the

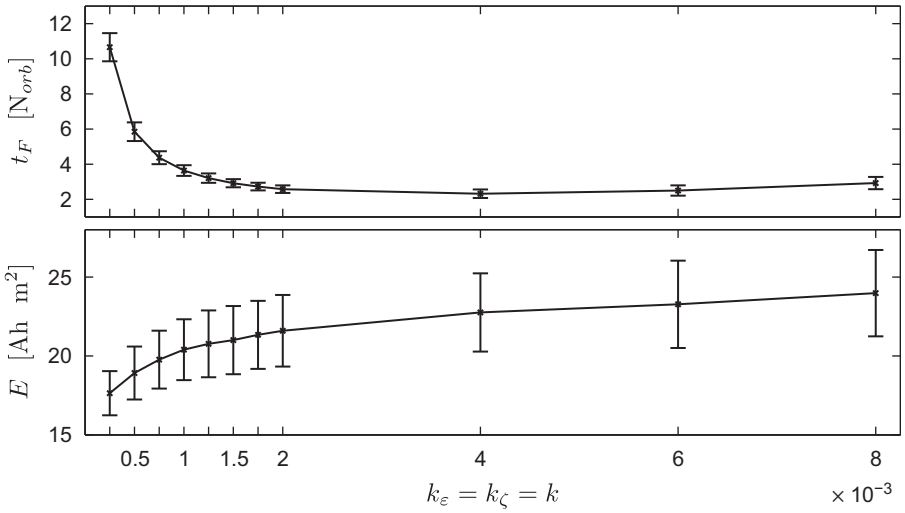

Fig. 2. Convergence time and electrical energy consumption of the test cases, as functions of $k_\varepsilon = k_\zeta = k$.

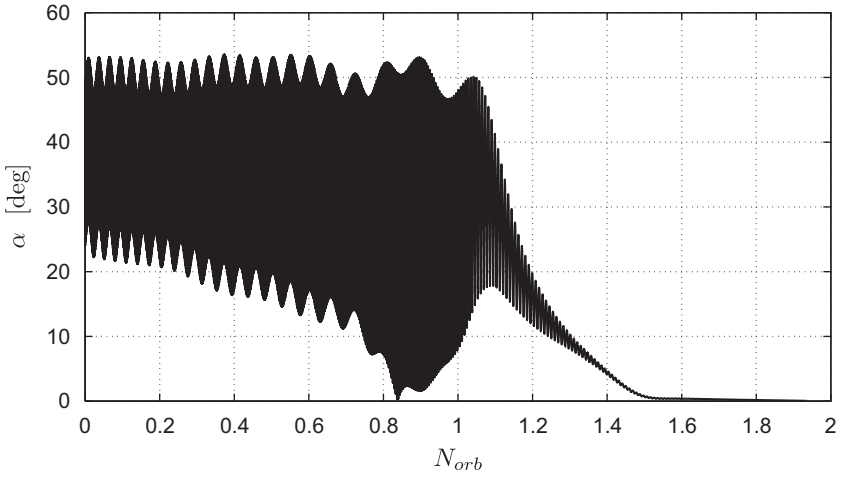

Fig. 3. Pointing error time history.

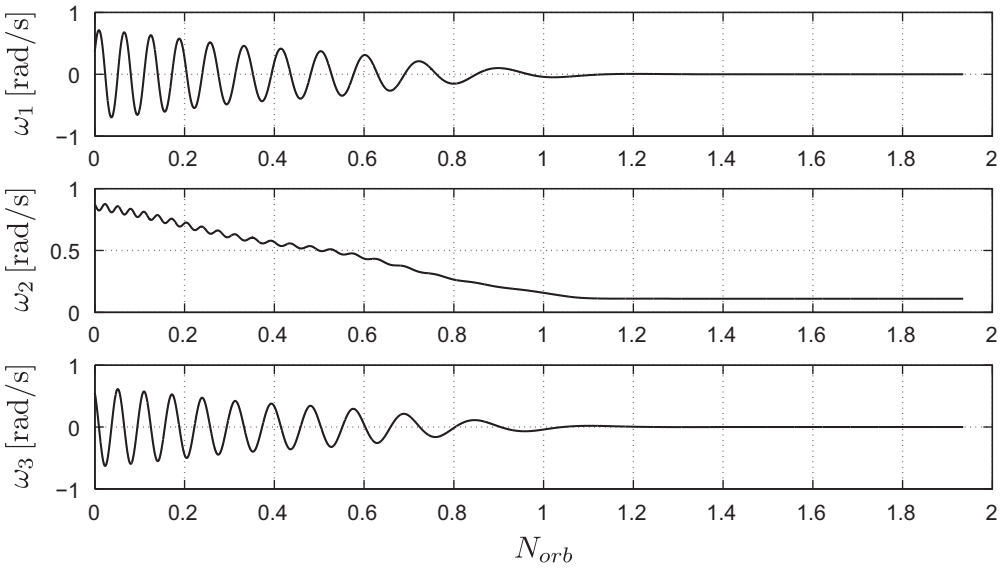

Fig. 4. Angular rates time history ($\boldsymbol{\omega}_d = (0,0.110,0)^T$ rad/s).

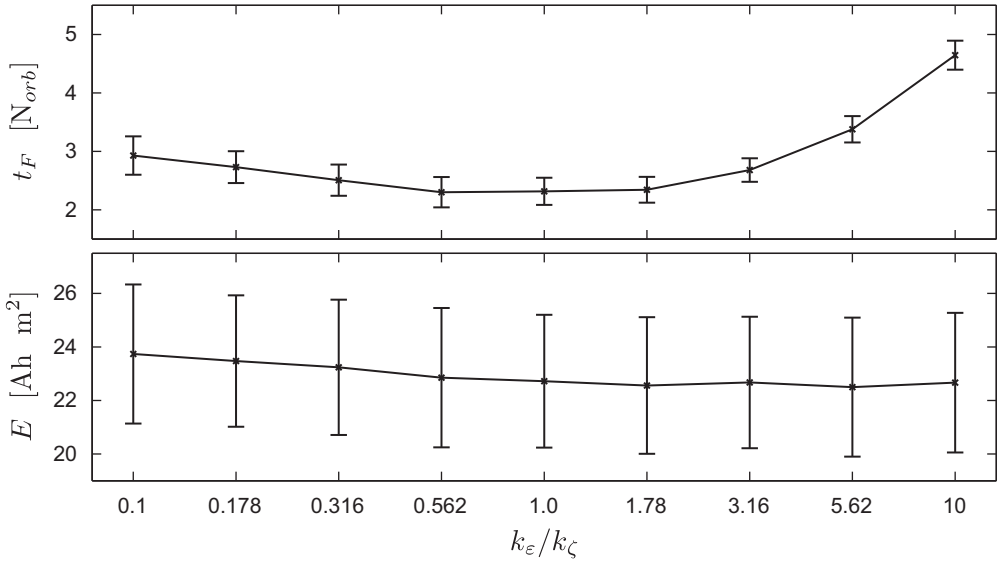

Fig. 5. Convergence time and electrical energy consumption of the test cases, as functions of $\log_{10}(k_\varepsilon/k_\zeta)$.

gains constant, that is, $k_\varepsilon + k_\zeta = 2k_{t_{min}}$, so that when $k_\varepsilon/k_\zeta = 1$ the best case of the previous set of Monte Carlo runs is recovered.

Fig. 5 shows that when the ratio k_ε/k_ζ is increased, the convergence time also increases significantly, becoming almost twice as much for $k_\varepsilon/k_\zeta = 10$. This behavior is due to the fact that the desired spin condition is rapidly reached and, at this point, gyroscopic stability makes it harder for the control system to stir the angular momentum vector toward the desired direction. Conversely, when k_ε becomes smaller and the term proportional to k_ζ becomes dominant, the angular momentum vector is aligned with the desired fixed direction $\hat{\boldsymbol{\sigma}}$ first, whereas the body-fixed spin-axis $\hat{\boldsymbol{e}}_2$ moves toward the same direction at a slower pace. Convergence time again increases, but less significantly, becoming only 40% higher than the minimum value for $k_\varepsilon/k_\zeta = 0.1$. This behavior is essentially due to gyroscopic cross-coupling terms in Euler equation, Eq. (1), which result into oscillations in the attitude variables that, in turn, maintain a higher average control power for reducing the remaining error signal around the three body axes. It is quite clear that best average convergence time are obtained around 1, for $0.562 < k_\varepsilon/k_\zeta < 1.78$.

As a final observation, the ratio k_ε/k_ζ apparently has a negligible effect on power expenditure, evaluated through the energy consumption parameter, E. This appears reasonable, provided that the sum of the gains is constant and higher gains are associated with higher levels of

required power. The increment for $k_\varepsilon/k_\zeta < 1$ is limited to approximately 4% of the average energy required for the reference case, $k_\varepsilon = k_\zeta = k_{t_{min}}$, and it is well within the dispersion interval defined by the standard deviation of E. In general, variations of k_ε/k_ζ do not represent an issue in the selection of control gains, as far as energy consumption is concerned, and $k_\varepsilon = k_\zeta = k$ thus results into a reasonable choice for the convergence characteristics demonstrated.

5. Conclusions

In this paper a control law based on the use of purely magnetic actuation for spin-stabilization is presented and discussed. It is shown that, with adequate orbit inclination, the control law globally exponentially stabilizes a three-inertial spacecraft, driving it toward a desired spin condition around a prescribed, yet arbitrary, axis fixed in the inertial frame. The proof extends a method developed for the acquisition of a pure spin around a principal axis of inertia, where the additional feature of aiming the spin axis in a desired direction is particularly relevant for practical applications.

The variability of the magnetic field along the orbit plays an important role in the proof of asymptotic stability of the system toward an equilibrium point (see Appendix). Monte Carlo simulation is used in order to confirm closed-loop stability and evaluate performance of the controller, showing a robust behavior with respect to the choice of the control gains and uncertainty on initial tumbling conditions.

Appendix A. Proof of global exponential stability

Global exponential stability of the origin $\boldsymbol{Y} = \boldsymbol{0}$ for the nominal system

$$\dot{\boldsymbol{Y}} = -\boldsymbol{A}(t)\boldsymbol{K}\boldsymbol{Y} \tag{30}$$

is provided by the following corollary.

Corollary 1. *Consider a non-linear non-autonomous dynamic system $\dot{\boldsymbol{x}} = \boldsymbol{f}(t,\boldsymbol{x})$, where $\boldsymbol{f} : \mathbb{R}^n \times \mathbb{R} \to \mathbb{R}^n$ is piecewise continuous in t and Lipschitz in $\boldsymbol{x}$. Let $\boldsymbol{x} = \boldsymbol{0}$ be an equilibrium point for the system at $t=0$. Also assume that a strictly positive definite Lyapunov-like function $V(\boldsymbol{x}) > 0$ exists, where (i) $V : \mathbb{R}^n \to \mathbb{R}$ is a smooth scalar function of the state $\boldsymbol{x}$ only and (ii) its gradient vanishes at the origin only, that is, $\nabla_x V = \boldsymbol{0}$ at $\boldsymbol{x} = \boldsymbol{0}$ and $\nabla_x V \neq \boldsymbol{0}$ elsewhere. If the Lyapunov-like function $V(\boldsymbol{x})$ and its time derivative $\dot{V}(t,\boldsymbol{x})$ satisfy the conditions*:

(1) $k_1\|\boldsymbol{x}\|^c \le V(\boldsymbol{x}) \le k_2\|\boldsymbol{x}\|^c \;\; k_1 > 0, \quad k_2 > 0, \quad c > 0$;
(2) *$\dot{V}$ is negative semi-definite, that is, $\dot{V}(t,\boldsymbol{x}) \le 0$*;
(3) *$\dot{V}$ is uniformly continuous*;
(4) *the iso-surfaces S of $V(\boldsymbol{x})$ in the state space $\mathbb{R}^n$ do not contain any integral curves $\boldsymbol{x}(t)$ of the vector field $\boldsymbol{f}$ other than the constant ones ($\boldsymbol{x}(t) = \boldsymbol{x}_e \quad \forall t$)*;

then the origin is exponentially stable.

Proof. Since the Lyapunov candidate function V only depends on the state $\boldsymbol{x}$ one has

$$\dot{V}(t,\boldsymbol{x}) = \lim_{\delta t \to 0} \frac{V(\boldsymbol{x}(t+\delta t)) - V(\boldsymbol{x}(t))}{\delta t} = \nabla_x V\, \boldsymbol{f}(t,\boldsymbol{x}) \tag{31}$$

Since the iso-surfaces S of $V(\boldsymbol{x}(t))$ do not contain any integral curves of $\boldsymbol{f}$, the right-hand term cannot be zero if an equilibrium point is not reached. Thus, for all $t > 0$ the quantity

$$V(\boldsymbol{x}(t+\delta t)) - V(\boldsymbol{x}(t)) = \int_t^{t+\delta t} \nabla_x V\, \boldsymbol{f}(\tau, \boldsymbol{x}(\tau,\boldsymbol{x}))\, \mathrm{d}\tau < 0 \tag{32}$$

is a finite negative term, and there exists a $0 < \lambda < 1$ such that

$$V(\boldsymbol{x}(t+\delta t)) - V(\boldsymbol{x}(t)) < -\lambda\, V(\boldsymbol{x}(t)) \tag{33}$$

From this point onwards the proof follows that of Theorem 8.5 in [24].

By choosing the Lyapunov candidate:

$$V(\boldsymbol{Y}) = 1/2\; \boldsymbol{Y}^T\boldsymbol{K}\boldsymbol{Y} \tag{34}$$

system (30) satisfies Conditions 1, 2, and 3, with

$$\dot{V}(t,\boldsymbol{Y}) = -(\boldsymbol{K}\boldsymbol{Y})^T\boldsymbol{A}(t)(\boldsymbol{K}\boldsymbol{Y}) \tag{35}$$

where $\boldsymbol{A}(t)$ is positive semi-definite. The Corollary can thus be applied if one demonstrates that Condition 4 also holds. From Eq. (35), it is clear that the time derivative of $V(t,\boldsymbol{Y})$ vanishes if one of the following conditions hold:

(1) The equilibrium point at the origin is reached, $(\boldsymbol{Z}^T,\boldsymbol{E}^T)^T = \boldsymbol{0}$ or
(2) The angular momentum error variables are such that the error signal, $\boldsymbol{e} = k_\zeta\boldsymbol{Z} + k_\varepsilon\boldsymbol{E}$, becomes parallel to the Earth magnetic field unit vector and the nominal torque $\boldsymbol{M}$ thus vanishes.

Suppose Condition 2 holds. As a matter of fact, in case of torque-free motion the nominal system (30) reduces to $\dot{\boldsymbol{Y}} = \boldsymbol{0}$, with the result that both $\boldsymbol{Z}$ and $\boldsymbol{E}$ remain fixed in the inertial frame. This condition can be maintained over time if and only if the vector $(k_\zeta\boldsymbol{Z}^T, k_\varepsilon\boldsymbol{E}^T)^T$ remains in the null-space of the time varying matrix, $\boldsymbol{A}$, $\mathcal{N}_A = \ker(\boldsymbol{A})$.

Letting $\boldsymbol{0} = (0,0,0)^T$, a basis for the null-space of $\boldsymbol{A}$ is given by the following four vectors, $\boldsymbol{n}_1 = (\boldsymbol{b}^T,\boldsymbol{0}^T)^T$, $\boldsymbol{n}_2 = (\boldsymbol{0}^T,\boldsymbol{b}^T)^T$, $\boldsymbol{n}_3 = (\boldsymbol{u}^T,-\boldsymbol{u}^T)^T$ and $\boldsymbol{n}_4 = (\boldsymbol{v}^T,-\boldsymbol{v}^T)^T$, where $\boldsymbol{u}$ and $\boldsymbol{v}$ are vectors perpendicular to $\boldsymbol{b}$. In other words, the vector $(k_\zeta\boldsymbol{Z}^T, k_\varepsilon\boldsymbol{E}^T)^T \in \mathcal{N}_A$ if $k_\zeta\boldsymbol{Z}$ and $k_\varepsilon\boldsymbol{E}$ have the same component along $\boldsymbol{b}$ and components opposite in sign on the plane perpendicular to $\boldsymbol{b}$, which means that the three vectors $k_\zeta\boldsymbol{Z}$, $k_\varepsilon\boldsymbol{E}$, and $\boldsymbol{b}$ must belong to the same plane.

Such a condition can be reached, but it cannot be maintained over a finite time-interval during a torque-free phase, as $\boldsymbol{b}$ either moves out of the plane identified by the two terms of the error vector or it rotates on the plane identified by them, thus changing their projections on the plane perpendicular to $\boldsymbol{b}$. This means that a trajectory $\boldsymbol{e}(t) = \|\boldsymbol{e}\|\hat{\boldsymbol{b}}(t)$ is not a solution for the nominal system (30). Thus, also Condition 4 is satisfied and the origin $\boldsymbol{Y} = \boldsymbol{0}$ is exponentially stable. □

References

[1] A.C. Stickler, K. Alfriend, Elementary magnetic attitude control system, J. Spacecr. Rockets 13 (5) (1976) 282–287.
[2] M. Lovera, A. Astolfi, Spacecraft attitude control using magnetic actuators, Automatica 40 (8) (2004) 1405–1414.
[3] M.J. Sidi, Spacecraft Dynamics and Control: A Practical Engineering Approach, Cambridge University Press, Cambridge, 1997.
[4] M. Grassi, M. Pastena, Minimum power optimum control of microsatellite attitude dynamics, J. Guidance Control Dyn. 23 (5) (2000) 798–804.
[5] F. Giulietti, A.A. Quarta, P. Tortora, Optimal control laws for momentum wheel desaturation using magnetorquers, J. Guidance Control Dyn. 29 (6) (2006) 1464–1468.
[6] B. Wie, P.M. Barba, Quaternion feedback for spacecraft large angle maneuvers, J. Guidance Control Dyn. 8 (6) (1985) 360–365.
[7] V. Coverstone–Carroll, Detumbling and Reorienting Underactuated Rigid Spacecraft, J. Guidance Control Dyn. 19 (3) (1996) 708–710.
[8] E. Silani, M. Lovera, Magnetic spacecraft attitude control: a survey and some new results, Elsevier, Control Eng. Pract. 13 (2005) 357–371.
[9] P. Tsiotras, J.M. Longuski, Spin-axis stabilization of symmetric spacecraft with two control torques, Syst. Control Lett. 23 (6) (1994) 395–402.
[10] H. Krishnan, N.H. McClamroch, M. Reyhanoglu, Attitude stabilization of a rigid spacecraft using two momentum wheel actuators, J. Guidance Control Dyn. 18 (2) (1995) 256–263.
[11] S. Kim, Y. Kim, Spin-axis stabilization of a rigid spacecraft using two reaction wheels, J. Guidance Control Dyn. 24 (5) (2001) 1046–1049.
[12] G. Avanzini, F. Giulietti, Constrained slews for single-axis pointing, J. Guidance Control Dyn. 31 (6) (2008) 1813–1816.
[13] M. Bosco, V. Fabbri, P. Tortora, ALMASat-EO attitude determination algorithms: evaluation, implementation and numerical simulation, in: Proceedings of the 8th International ESA Conference on Guidance and Navigation Control Systems, Carlsbad, Czech Republic, 5–10 June 2011.
[14] Y.J. Cheon, S.H. Lee, J.H. Kim, Fully magnetic devices-based control for gyroless target pointing of a spinning spacecraft, IEEE Trans. Aerosp. Electron. Syst. 46 (3) (2010) 1484–1491.
[15] A. de Ruiter, A fault-tolerant magnetic spin stabilizing controller for the JC2Sat–FF Mission, Acta Astronaut. 68 (2011) 160–171.
[16] G. Avanzini, E.L. de Angelis, F. Giulietti, Acquisition of a desired pure spin condition for a magnetically actuated spacecraft, J. Guidance Control Dyn, in press.
[17] Zh.S. Athanassov, Perturbation theorems for nonlinear systems of ordinary differential equations, J. Math. Anal. Appl. 86 (1982) 194–207.
[18] S. Elaydi, H.R. Farran, Exponentially asymptotically stable dynamical systems, Applicable Anal. 25 (1987) 243–252.
[19] S.K. Choi, K.S. Koo, K. Lee, Lipschitz stability and exponential asymptotic stability in perturbed systems, J. Korean Math. Soc. 29 (1) (1992) 175–190.
[20] J.R. Wertz, Spacecraft Attitude Determination an Control, Kluwer Academic Publishers, Dordrecht, Holland, 1978.
[21] H.B. Hablani, Comparative stability analysis and performance of magnetic controllers for bias momentum satellites, J. Guidance Control Dyn. 18 (6) (1995) 1313–1320.
[22] B. Wie, Space Vehicle Dynamics and Control, American Institute of Aeronautics and Astronautics Inc., Reston, VA, 1998 (Chapter 7).
[23] G. Avanzini, F. Giulietti, Magnetic detumbling of a rigid spacecraft, J. Guidance Control Dyn. 35 (4) (2012) 1326–1334. July–August.
[24] H.K. Khalil, Nonlinear Systems, Third edition, Prentice–Hall, Upper Saddle River, New Jersey 07458, 2001.